Jeomorfolojik Araştırmalar Dergisi
Journal of Geomorphological Researches
© Jeomorfoloji Derneği www.dergipark.gov.tr/jader E - ISSN: 2667 - 4238

Araştırma Makalesi / Research Article

FLOOD SUSCEPTIBILITY MAPPING IN THE DRAINAGE BASINS OF THE GULF OF İSKENDERUN (TÜRKİYE) USING MORPHOMETRIC AND MULTIVARIATE TECHNIQUES

Morfometrik ve Çok Değişkenli Teknikler Kullanılarak İskenderun Körfezi (Türkiye) Drenaj Havzalarında Taşkın Duyarlılık Haritalaması

Mustafa UTLU[a], Redvan GHASEMLOUNIA[b], Semir DEMİRBİLEK[c]

[a] Burdur University, Faculty of Science and Letter, Department of Geography, Burdur Türkiye
utlumus@gmail.com https://orcid.org/0000-0002-7508-4478
[b] Sorumlu Yazar / Corresponding Author
Istanbul Gedik University, Engineering Faculty, Department of Civil Engineering, Istanbul, Türkiye
redvan.ghasemlounia@gedik.edu.tr https://orcid.org/0000-0003-1796-4562
[c] Hatay Mustafa Kemal University, Department of Geography, Faculty of Arts and Sciences, Hatay, Türkiye
semirdemirbilek@mku.edu.tr https://orcid.org/0000-0003-4463-4016

Makale Tarihçesi
Geliş 24 Eylül 2025
Kabul 14 Ekim 2025

Article History
Received 24 September 2025
Accepted 14 October 2025

Anahtar Kelimeler
Normalize Edilmiş Morfometrik Taşkın İndeksi (NMFI), Temel Bileşen Analizi (PCA), Duyarlılık Haritalaması, Taşkın, Taşkın Yönetimi

Keywords
Normalised Morphometric Flood Index (NMFI), Principal Component Analysis (PCA), Susceptibility Mapping, Flood, Flood Management

Atıf Bilgisi / Citation Info
Utlu, M., Ghasemlounia, R. & Demirbilek, S. (2025) Flood Susceptibility Mapping in the Drainage Basins of the Gulf of İskenderun (Türkiye) Using Morphometric and Multivariate Techniques, Jeomorfolojik Araştırmalar Dergisi / Journal of Geomorphological Researches, 2025 (15): 170-188.

doi: 10.46453/jader.1790383

ABSTRACT

Floods, whose frequency and severity have increased due to both climate change and anthropogenic effects such as urbanization, deforestation, and land use changes, continue to pose serious risks to human life, infrastructure, and ecosystems worldwide. In regions like southern Türkiye, where complex topography, orographic precipitation, and rapid urban growth intersect, understanding flood dynamics is particularly critical. This study evaluates the flood susceptibility of 24 river basins that drain into the Gulf of İskenderun, focusing on the districts of Erzin, Dörtyol, İskenderun, Arsuz and Belen in Hatay Province. In this study, we developed a comprehensive framework for assessing spatial flood risk by integrating morphometric analysis with statistical classification methods. Fourteen morphometric parameters derived from 10-meter resolution digital elevation models were processed using GIS-based analyses. The proposed methodology involves two complementary analytical techniques: the Normalized Morphometric Flood Index (NMFI) and Principal Component Analysis (PCA). The Normalized Morphometric Flood Index (NMFI) plays a significant role in understanding and identifying flood-prone basins. This method allows the morphometric-based evaluation results of flood-prone basins to be normalized, enabling the obtained values to range between 0 and 1, and classifying flood susceptibility into four distinct categories. The Principal Component Analysis (PCA), on the other hand, considers the dynamic parameters influencing the occurrence of flood events and highlights the most dominant and effective parameters contributing to flooding. As a result of evaluating 24 river basins draining from the Amanos Mountains into the İskenderun Gulf, it was found that, although some differences exist between the two methods, both approaches identified several basins with high flood-generation potential and exhibited many similarities. Moreover, a portion of these 24 basins was classified within the moderate and high flood susceptibility categories. Furthermore, the results derived from the PCA method demonstrated superior performance compared to the NMFI method in terms of classification accuracy, recall rate, and overall reliability. According to the analysis, the drainage density (D_d), bifurcation ratio (R_b), time of concentration (T_c), circularity ratio (R_c), and basin relief (B_h) were identified as the most influential factors affecting flood potential across the 24 basins. The findings from both methods reveal that these approaches are critically important for understanding flood potential and identifying flood-prone basins. Moreover, they can be effectively applied to small-, medium-, and large-scale basins. These results are particularly valuable for conducting rapid and probabilistic assessments in watersheds and support hydraulic modeling-based flood hazard and risk analyses in areas with high flood potential, thereby contributing to a more efficient decision-support process in flood management.

1. INTRODUCTION

Floods, directly influenced by climate change, are among the most destructive and frequent natural disasters. Throughout history, they have caused profound social, economic, and environmental impacts worldwide (Haltas et al., 2021). Flood events, which in the past mostly occurred on a local scale and for short durations (Trenberth, 2011), have now turned into catastrophic extreme flood disasters affecting much larger areas due to atmospheric currents, prolonged heavy rainfall, and increases in temperature events (Milly et al., 2002). Certainly, this situation is directly linked to incorrect engineering practices on riverbeds, urbanization, the increasing prevalence of impermeable surfaces, and rapid and sudden changes in land cover (Milly et al., 2002; Tayanç et al., 2009; Youssef et al., 2011; Aydin & Raja, 2020). Therefore, floods experienced today have evolved from being merely a result of hydrological and geomorphological processes to becoming more complex, more frequent, and more destructive due to the impact of human activities (Alifujiang et al., 2021).

The number and severity of flood events occurring in almost every geography across the world are increasing on a global scale (Hirabayashi et al., 2008, 2013). Flood events, which cause billions of dollars in economic losses each year, also result in the deaths of thousands of people. According to the WHO, over 2 billion people were affected by floods between 1998 and 2017 (Kowalzig, 2008; Özay & Orhan, 2023; Balcı et al., 2024). Until 2008, flood events affected an average of 100 million people, but by 2016, this number had increased to 250 million, following a growing trend (OECD ,2016; Balcı et al., 2024). Future projections, based on observed changes in climate patterns, suggest that the impact of floods will increase even further in the coming years. Indeed, it is expected that by 2050, around 450 million people and 430 thousand square kilometers of agricultural land will be affected by floods (Arnell & Gosling, 2016). In this context, the economic loss caused by floods and other water-related disasters on a global scale is projected to reach 5.6 trillion dollars (Dickie, 2022). Especially countries with high population density, such as China, India, and Bangladesh, rank among the most affected by floods. On the other hand, the countries most affected in proportion to their population are the Netherlands (59%), Bangladesh (58%), and Vietnam (46%) (Rentschler et al., 2022).

Due to Türkiye's climatic characteristics, geographic location, topographical, and geological features, it is one of the countries most exposed and sensitive to flood events, with an average of 18 flood events occurring each year (Yüksek et al., 2013; Koç et al., 2020; Utlu, 2023). The resulting damage averages 86 million dollars annually (DSI, 2012; Yüksek et al., 2013). In addition to the physical geography conditions, the increasing population and urbanization in recent years, or in short, anthropogenic factors, have led to an increase in both the frequency and severity of flood events. As a result, the damage and problems caused by floods have also rapidly escalated. Flood events in Turkey occur under different parameters in different regions, with intense flooding mainly occurring in the Mediterranean and Black Sea regions, although there have been noticeable catastrophic flood events in other regions in recent years. According to the study by Gürer & Uçar, (2009) between 1955 and 2009, there were 2,089 flood events, resulting in the loss of 1,360 lives, affecting an area of over 2 million hectares, and causing damage exceeding 3 billion dollars (Utlu et al., 2020).

One of the key methods for assessing flood susceptibility is drainage basin morphometry. This approach provides quantitative information based on the areal, relief, and drainage characteristics of basins, aiding in the understanding of their flood-generating potential and enabling the rapid mitigation of potential economic and social impacts. Numerous studies have been conducted worldwide, including in Turkey, on drainage basin morphometry at global, regional, and smaller watershed scales (Utlu & Ghasemlounia, 2021; Enea et al., 2024; Demirbilek & Turoğlu, 2025). Various morphometric indices have been developed to evaluate the flood-generating potential of basins based on their areal, relief, and drainage characteristics. In recent years, the application of this method has provided effective results for both integrated basin management and the assessment of flood susceptibility, while also facilitating timely and critical mitigation measures. Overall, basin morphometry is widely used to analyze both the flood-generating potential of sub-watersheds that feed main rivers and the flood risks within the main river basins themselves (Bhat et al., 2019; Rai et al., 2020; Telore, 2020; Tukura et al., 2021; Ghasemlounia & Utlu, 2021). For instance, Alam et al. (2021) conducted a study in southeastern Bangladesh, evaluating 13 sub-watersheds using 18 different morphometric indices based on SRTM DEM data. Their study identified the B4 and B6 sub-watersheds as belonging to the "very high" flood susceptibility class, while the other watersheds were classified into different flood susceptibility categories. Moreover, the study highlighted that the Topographic Wetness Index (TWI) and Topographic Position Index (TPI) significantly contributed to the assessment of flood susceptibility. El-Fakharany & Mansour (2021) evaluated the flood potential of the Wadi Al Aawag basin in the southwestern Sinai region of Egypt using basin morphometry. Their findings indicated that sub-basins with high topographic relief, impermeable lithological characteristics, and short flow concentration times exhibited high flood potential and susceptibility. Additionally, the study emphasized that surface topography and the final drainage network play a critical role in surface runoff and flood generation.

The present study aims to understand flood dynamics and the flood-generating potential of 24 river basins originating from the Amanos Mountains and draining into the İskenderun Gulf, which exhibit diverse geometries and substantial areal variability. Based on the analysis results, the flood-generating potential of the basins was evaluated using the Normalized Morphometric Flood Index (NMFI) and Principal Component Analysis (PCA). Fourteen morphometric indices, reflecting areal, linear, and relief-based morphometry, were employed to comprehensively assess the basins. Accordingly, morphometric analyses were conducted in 24 different river basins, and their accuracy was tested by validating the results with historical flood events. The study compares the outcomes of both methods and discusses which approach yields more reliable results in terms of flood susceptibility.

2. METHODOLOGY

2.1. Study Area

This study focuses on the morphometric and hydrological characteristics of 24 river basins that drain into the Asi River, specifically within the districts of Erzin, Dörtyol, İskenderun, and Belen in Hatay Province, southern Türkiye (Figure 1(a) and 1(b). These basins exhibit a wide range of geometric forms, with areas varying between 4.1 km^2 and 289.1 km^2. Their perimeters range from 13.1 km to 135.4 km, reflecting significant variability in basin shapes. The minimum elevations within the basins range from sea level (0 m) to 2,240 m, indicating diverse topographic conditions. Land cover analysis based on ESA's WorldCover 2021 (Url-1) dataset (10 m spatial resolution) reveals that the study area is predominantly covered by forest, with tree cover accounting for approximately 73.5% of the total basin area. Grasslands represent the second most widespread class at 12.3%, followed by croplands (5.9%), built-up areas (3.7%), shrubland (3.3%), and bare or sparsely vegetated surfaces (1.3%), (Figure 1c). Spatially, forest cover is primarily concentrated in the higher elevations of the Amanos Mountains, especially within the Belen district and surrounding mountainous terrain. In contrast, croplands, grasslands, and urbanized areas are predominantly distributed across the lower elevations and flatter regions of Erzin, Dörtyol, Arsuz and İskenderun, where both settlement and agricultural activity are more prominent due to favorable topographic conditions. This variation in land cover types plays a crucial role in surface runoff behavior and the hydrological response of each basin, particularly in relation to flood potential and infiltration dynamics.

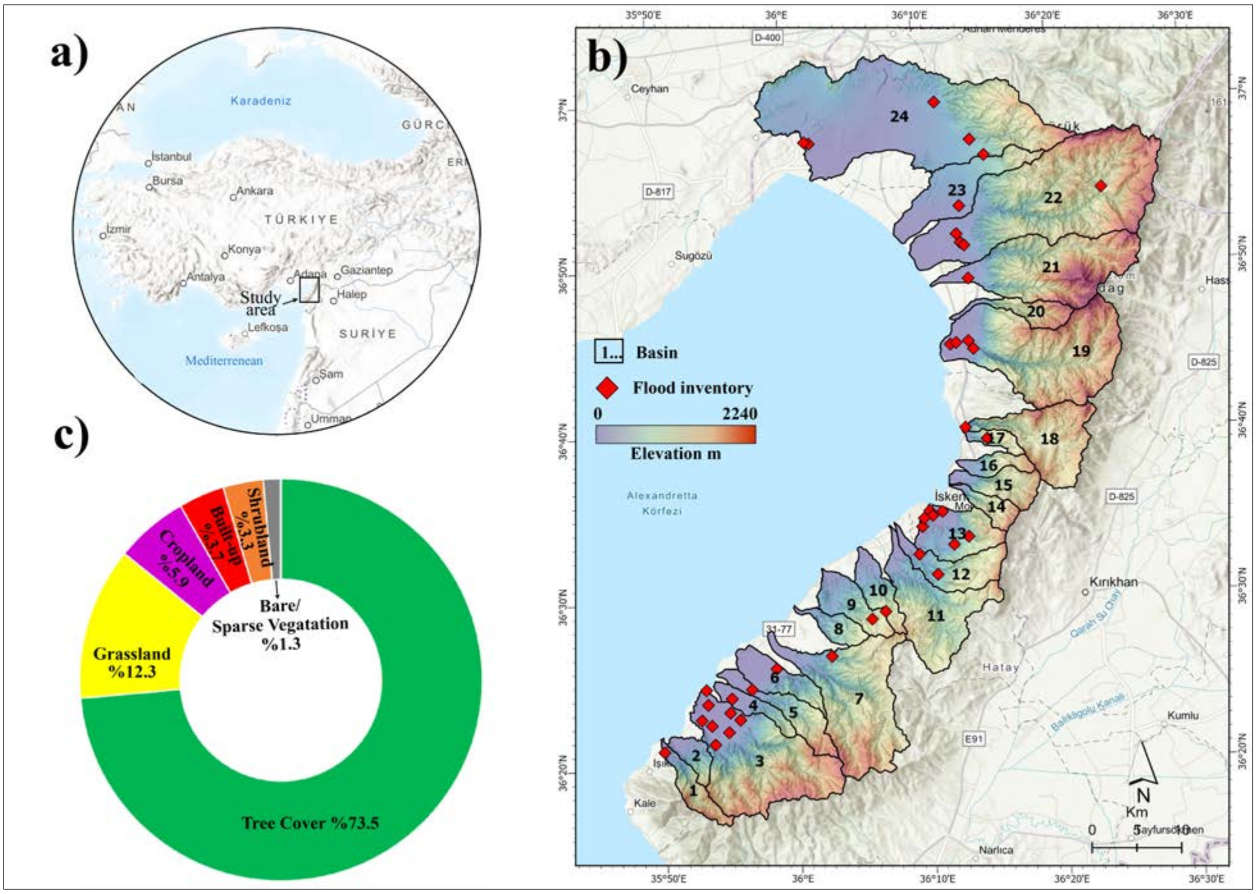

Figure 1: a) The location of the study area b) distribution of the basins and flood inventory c) distrubiton of the landcover type of the basin based on ESA-Worldcover 2021 (Url -1).

Basins are almost entirely contained within Hatay's provincial boundaries and ultimately discharge into the Mediterranean Sea through the İskenderun Gulf, a coastal region influenced by both marine and orographic climatic dynamics. According to Taşoğlu et al. (2024), the region is classified as a "C" type temperate climate zone under the Köppen-Geiger classification system. Subtypes include "Csa" (hot-summer Mediterranean climate) in low-lying and coastal areas, and "Csb" (warm-summer Mediterranean climate) in the higher mountainous zones. The climate is characterized by hot and dry summers, with an average annual temperature of approximately 16°C. Annual precipitation ranges between 721 mm and 915 mm, with the majority of rainfall occurring from November to May. In contrast, the summer months receive minimal precipitation, averaging only around 8 mm.

2.2. Data Source

In this study, a 10-meter resolution Digital Elevation Model (DEM) derived from a 1:25,000 scale topographic map was used. Accordingly, all analyses conducted within the scope of the study were carried out based on the TOPO-DEM data. The data used in watershed-based morphometric analyses and the determination of flood generation potentials, as well as the overall flowchart of the study, are presented in Figure 2. All spatial data in this study were processed using the WGS84 datum and the Universal Transverse Mercator (UTM) projection within Zone 36. In addition, geomorphometric characteristics of the basins were analyzed using Geographic Information System (GIS) technologies, primarily ArcGIS Pro 3.5.2. For the interpretation and statistical evaluation of the outputs, Microsoft Excel and SPSS software were employed.

2.3. Morphometric Parameters

In this study, the flood potential of 24 river basins located to the west of the Amanos Mountains and draining into the Mediterranean Sea via the Gulf of İskenderun was assessed through basin-scale flood morphometry. A total of 16 morphometric indices were applied to each basin and classified into three major groups: linear, areal, and relief morphometric parameters (Table 1).

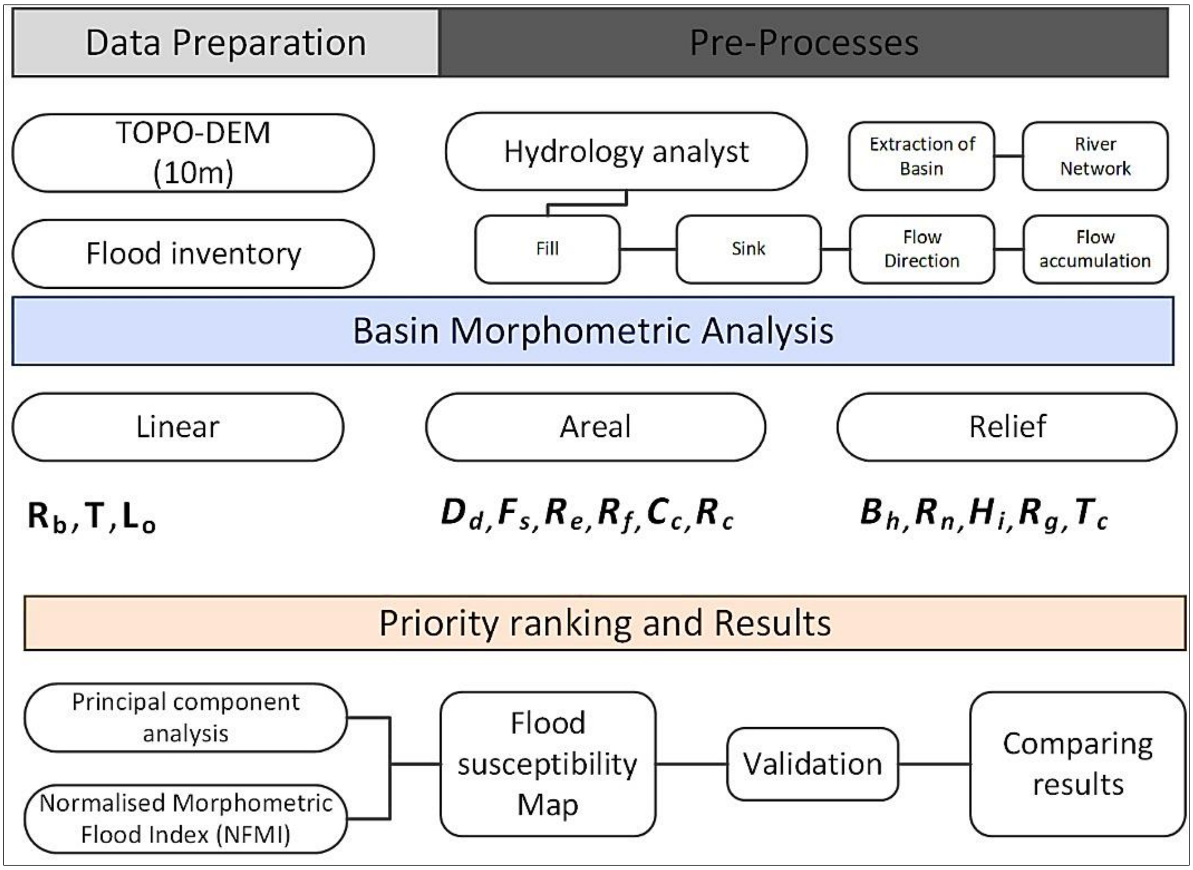

Figure 2: General flowchart of the study.

Linear aspect included: Stream length ratio (R_l), Bifurcation ratio (R_b), Length of overland flow (L_o), Texture ratio (T),

Areal aspect included: Drainage density (D_d), Stream frequency (F_s), Elongation ratio (R_e), Form factor (R_f), Compactness coefficient (C_c), Circularity ratio (R_c),

Relief aspect included: Basin relief (B_h), Relief ratio (R_h), Ruggedness number (R_n), Hypsometric integral (H_i), Gradient ratio (R_g), and Time of concentration (T_c).

Table 1: Morphometric parameters for NMFI index

No	Morphometric parameters	Mathematical expression	References
	Basic aspect		
1	Area (A)	Area of basin (km2) GIS Analysis	Horton(1945)
2	Stream order (u)	Strahler stream order. Hierarchical rank	Strahler(1964)
3	Total number of stream (N)	Total number of streams in basin	Strahler(1958)
4	Total number of each order Nu (1,2,3,..)	Total number of streams of each order	Horton(1945)
5	Total length of stream (L)	Total length of stream	Horton(1945)
6	Total length of each order L_u (1,2,3,...)	Total length of each order	
7	Maximum elevation (H_{max})	Maximum elavation of basin	
8	Minimum elevation (H_{min})	Minimum elavation of basin	
9	Mean elevation (H_{mean})	Mean elavation of basin	
	Linear param.		
10	Bifurcation ratio (R_b)	$Nu=N_u/(N_u+1)$	Horton(1945)
11	Stream length ratio (R_l)	$R_l=L_u/(L_u+1)$	Strahler(1964)
12	Length of overland flow (L_o)	$Lo=1/2D_d$	Horton(1945)
13	Texture ratio (T)	T=N1/P	Smith(1950)

	Areal aspect		
14	Drainage density (D_d)	D_d=L/A	Horton(1945)
15	Stream frequency (F_s)	F_s=N/A	Horton(1945)
16	Form factor (R_f)	R_f=A/Lb2	Horton(1932)
17	Elongation ratio (R_e)	Re=(2/L_b)*(A/π)$^{0.5}$	Schumm(1956)
18	Compactness coeefficient (C_c)	0.2841P/A05	Gravelius(1914)
19	Circularity ratio (R_c)	Rc=4πA/P	Miller(1953)
	Relief aspect		
20	Basin relief (B_h)	B_h=H_{max}-H_{min}	Schumm(1956)
21	Relief ratio (R_h)	R_h=H/L	Schumm(1956)
22	Ruggedness number (R_n)	R_n=B_h*D_d	Melton(1957)
23	Hysometric integral (*Hi*)	Hi=(H_{mean}-H_{min})/H_{max}-H_{min})	Pike and Wilson(1971), Mayer (1990)
24	Gradient ratio (R_g)	Rg=(Z-z)/L	Sreedevi(2004)
25	Times of Concentration (T_c)	T_c= 0.0195.L0.77.S-0.385	Kirpich(1940)

2.4. Morphometric Flood Susceptibility Analysis Using NMFI and PCA Integration

Several contemporary approaches are commonly employed to evaluate factors influencing basin-scale flood events, including hydraulic and hydrologic modeling, susceptibility models, and morphometric analyses. Among these, morphometric analysis provides valuable insights into flood potential by quantifying drainage networks, basin geometry, and relief characteristics. This method plays a particularly critical role in basins where streamflow observation stations are lacking or where high-resolution and detailed digital elevation models required for hydrological modeling are unavailable. In this study, morphometric indices were used in combination with the Normalized Morphometric Flood Index (NMFI) and Principal Component Analysis (PCA) to statistically enhance the interpretation of results and assess flood susceptibility across 24 river basins.

2.5. Normalized Morphometric Flood Index (NMFI) Calculation

The NMFI method was first developed by Özdemir and Akbaş (2023). Within the framework of drainage basin morphometry, this method evaluates the flood susceptibility potential based on each morphometric parameter under areal, linear, and relief morphometry. Briefly, each parameter used across the three morphometric categories is normalized to a 0–1 range, which allows for objective comparison across different basins and eliminates subjective interpretation during analysis. This approach fundamentally provides more reliable and comparable results. The method varies depending on the flood-generating potential of each parameter. For morphometric indices where higher values indicate a greater likelihood of flooding, Equation (1) is applied, whereas for parameters where lower values correspond to higher flood potential, Equation (2) is used.

$$NMFI = \frac{1}{n}\sum_{i=1}^{n}\left(\frac{m_i - mi_{min}}{mi_{max} - mi_{min}}\right) \qquad (1)$$

$$NMFI = \frac{1}{n}\sum_{i=1}^{n}\left(\frac{m_i - mi_{max}}{mi_{min} - mi_{max}}\right) \qquad (2)$$

In this equation, **mi_min** and **mi_max** represent the minimum and maximum values obtained from the applied morphometric indices, **n** denotes the total number of morphometric indices used, and **mi** indicates the value obtained from the respective index (Özdemir & Akbaş, 2023).

After normalization, each basin is assigned a mean NMFI value, which reflects its overall flood susceptibility. These values are then classified into four categories presented in the Figure 3.

According to this method, the final value obtained for each result, along with the average of the total parameters in the basin, allows for the systematic derivation of susceptibility data or outcomes based on the parameters used and the morphometric characteristics of the basins.

2.5. PCA-Based Flood Susceptibility

This approach is one of the actively employed methods in contemporary flood susceptibility modeling. The flood susceptibility results derived from the NMFI (Normalized Morphometric Flood Index) method were also evaluated through Principal Component Analysis (PCA). Due to the high number of parameters used in the NMFI method and the significant intercorrelation among them, PCA was preferred as a technique that reduces the dimensionality of the dataset by transforming correlated variables into a smaller number of independent components while preserving most of the data's variance. In this study, PCA was applied to 16 morphometric parameters. The first principal component (PC1), which explained the largest portion of the variance, was primarily considered, followed by the second (PC2) and third (PC3) components. During this process, highly correlated parameters were identified, and based on the loading values of the selected components, the NMFI values were weighted to generate a composite flood susceptibility score for each basin. The resulting scores were then used to produce the final flood susceptibility ranking for each basin. The integrated approach combining NMFI and PCA facilitated a more objective and data-driven classification by reducing redundancies and multicollinearity between the morphometric indices.

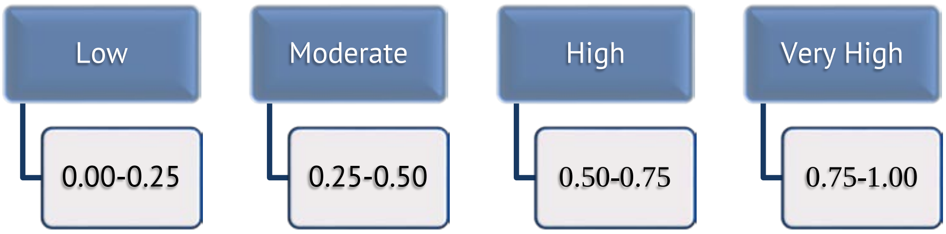

Figure 3: Basin overall flood susceptibility mean NMFI categories (Ozdemir & Akbas 2023).

3. FINDINGS

3.1. Linear Parameters

3.1.1. Bifurcation ratio (R_b)

The bifurcation ratio (R_b) represents the ratio of streams from one order to the next higher order. Lower R_b values indicate higher surface runoff and, consequently, a higher flood potential, whereas higher R_b values correspond to lower flood-generating potential (Bashir & Alsalman, 2024). In the analysis of 24 river basins, Rb values ranged from 1.63 to 4.05. The basin with the lowest Rb value (basin 24) exhibits a high flood-generating potential, while the basin with the highest Rb value (basin 12) shows a lower flood-generating potential. According to the NMFI classification, 1 basin falls under the low susceptibility class, 2 basins under the high susceptibility class, and 21 basins under the very high susceptibility class (Figure 4).

3.1.2. Length of overland flow (L_o)

The length of overland flow (L_o) represents the delay of water movement during the surface runoff process (Horton, 1945). L_o is inversely related to drainage density. Lower L_o values increase flood risk, whereas higher L_o values indicate lower flood potential (Kumar Rai et al., 2017). In the 24 river basins analyzed, L_o values ranged from 0.002 to 0.130. The lowest L_o value was observed in basin 24, where the R_b value was also low, indicating a high flood potential. Conversely, the highest L_o value was found in basin 20, which represents the lowest flood potential. According to the NMFI classification, 5 basins have low, 1 basin has moderate, 5 basins have high, and 13 basins have very high flood susceptibility (Figure 4).

3.1.3. Texture ratio (T)

It is the ratio of the total number of first-order stream segments within a river basin to the perimeter length of the basin. (Alam et al., 2021; Ghasemlounia & Utlu, 2021). Higher T values indicate a finer drainage texture, often linked to quicker runoff and higher flood risk (Arabameri et al., 2020). In this study, texture ratio values varied between 9.0 and 43.9. The highest value (43.9) was found in basin 22, suggesting a very fine drainage texture and a strong tendency for rapid surface runoff. The lowest value (9.0) was observed in basin 16 potentially lower flood susceptibility. According to NMFI method 14 basins the low (0.00–0.25), 5 basins are moderate (0.25–0.50), 3 basins are high (0.50–0.75), and 2 basins are very high susceptibility (0.75–1.00; Figure 4).

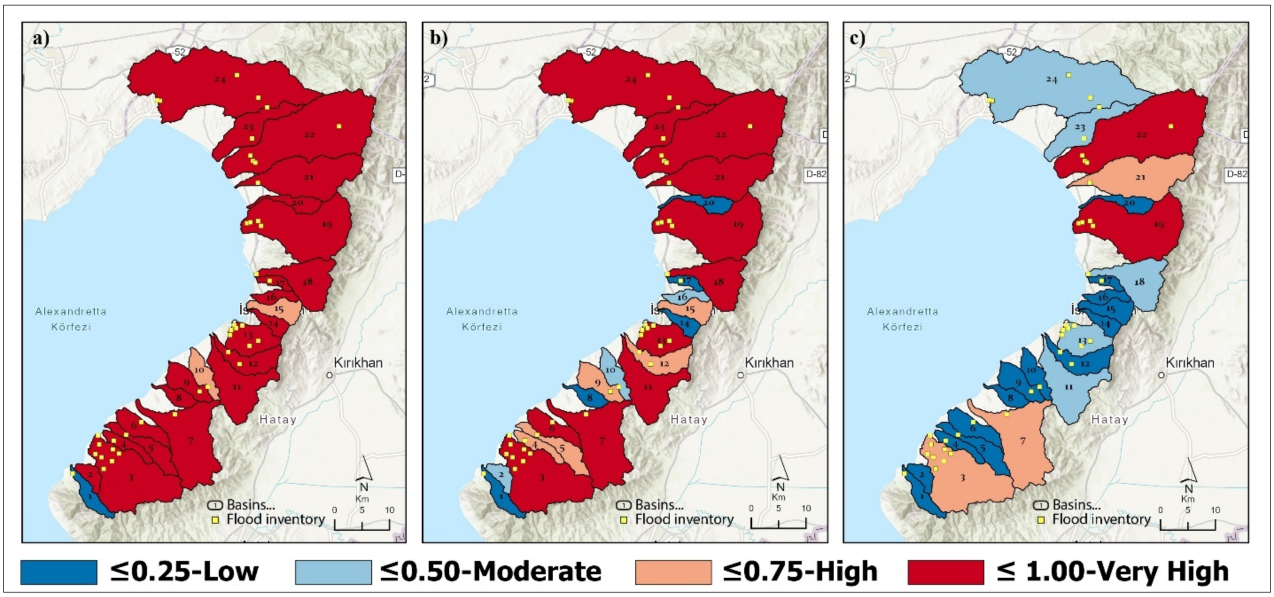

Figure 4: Normalised value distributions of the linear morphometric parameters a) R_b, b) L_o, and c) T evaluated for the flood-generating potential of the İskenderun Körfezi River basins.

3.2. Areal Parameters

3.2.1. Drainage density (D_d)

Higher drainage density represents a more dissected basin and faster runoff, often leading to increased flood potential (Horton, 1945; Farhan et al., 2017). Lower values show slower water movement and greater infiltration potential (Bashir & Alsalman, 2024). In this study, drainage density values varied between 2.77 and 20.14 km/km². The highest value (20.14) was observed in basin 24, indicating a dense and highly dissected drainage network prone to rapid flood response. The lowest value (2.77) was recorded in basin 20, implying a lower channel density and potentially slower runoff. 17 basins were classified within the low (0.00–0.25), 1 basin was classified under moderate (0.25–0.50), 5 basins were classified as high (0.50–0.75), and 1 basin fell into the very high susceptibility category (0.75–1.00; Figure 5).

3.2.2. Stream frequency (F_s)

It is a crucial indicator for runoff potential. Higher stream frequency suggests a more active drainage system with greater potential for quick runoff and flooding, while lower values indicate reduced drainage activity and slower hydrologic response (Horton, 1945; Obeidat et al., 2021). In this study, stream frequency values ranged from 11.63 to 56.8. The highest value (56.8) basin 22 reflecting an intensely dissected terrain with high flood susceptibility. The lowest value (11.63) in basin 17, indicating less drainage intensity and a relatively lower flood response. In the analysis of the 24 basins, the results based on the NMFI classification: 14 basins are classified as low (0.00–0.25), 4 basins are classified as moderate (0.25–0.50), 3 basins are classified as high (0.50–0.75), and 3 basins are classified as very high susceptibility (0.75–1.00; Figure 5).

3.2.3. Elongation ratio (R_e)

Elongation ratio quantifies the degree to which a basin's shape (Horton, 1932) approaches that of a circle. It is calculated based on the relationship between the basin area and its maximum length (Schumm, 1956). R_e is positively correlated with flood susceptibility. Generally, more circular and compact basins allow precipitation to reach the drainage network more rapidly, thereby shortening the concentration time and increasing the likelihood of flash flooding (Sutradhar & Mondal, 2023). In contrast, elongated basins tend to disperse runoff over a longer period, reducing peak discharge and flood potential. In the current analysis, R_e values are ranged from

0.01 to 0.11 across the studied basins. Basin 24, with the lowest Re value (0.01), represents a highly elongated morphology and is considered one of the least flood-prone basins. On the other hand, Basin 2, with the highest Re value of 0.57, has a more circular and compact shape. This indicates a higher potential for flooding. based on the Re values of the 24 basins, the NMFI classification results are as follows: 10 basins the low, 8 into the moderate, 4 into the high, and 2 basins into the very high flood susceptibility class (Figure 5).

3.2.4. Form factor (R_f)

Form factor is an important morphometric parameter used to determine the geometric characteristics (circular or elongated) of drainage basins (Strahler 1964). While high R_f values indicate more circular basin geometries and are positively correlated with flood potential, lower R_f values represent more elongated basins, which are generally associated with lower flood potential (Telore, 2020; Mishra & Rai, 2020). In the 24 basins R_f values range from 0.36 to 0.89. Basin 22 has the highest Rf value (0.89), while Basin 24 has the lowest value (0.36). The NMFI classification of R_f in the 24 basins reveals the following distribution in terms of flood susceptibility: 4 basins are classified as low susceptibility (0.00–0.25), 11 basins are classified as moderate susceptibility (0.25–0.50), 5 basins are classified as high susceptibility (0.50–0.75), and 4 basin is classified as very high susceptibility (0.75–1.00; Figure 5).

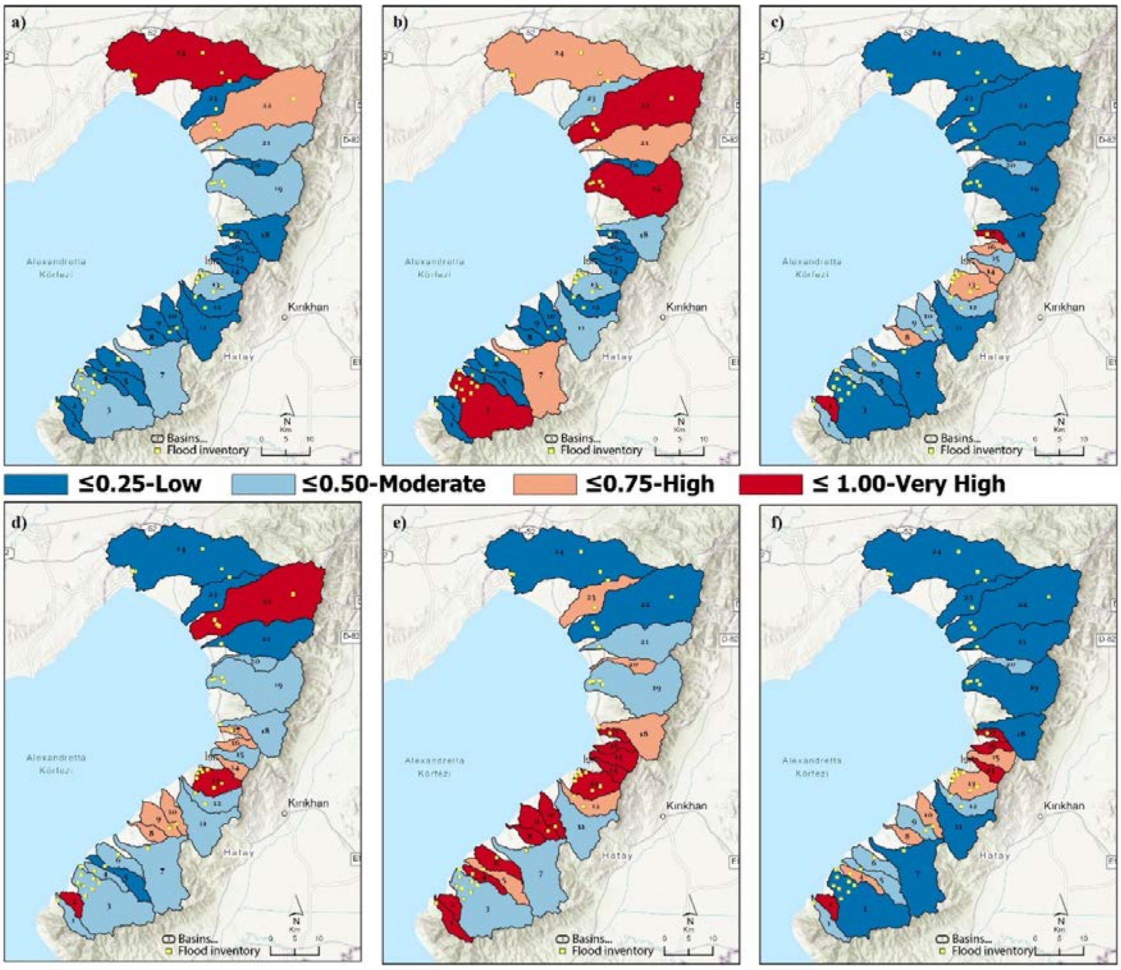

Figure 5: Normalised value distributions of the areal morphometric parameters a) D_d , b) F_s , c) R_e , d) R_f , e) C_c , and f) R_c evaluated for the flood-generating potential of the İskenderun Körfezi River basins.

3.2.5. Circularity ratio (R_c)

Circularity ratio is a morphometric parameter that quantifies how circular a drainage basin is. The closer the R_c value is to 1, the more circular the basin shape, which typically leads to faster runoff concentration and higher flood susceptibility. Conversely, a lower R_c value suggests a more elongated or irregular basin shape, which results in slower runoff concentration and a reduced flood risk. Basin

24, with the minimum R_c value of 0.09, represents the most elongated or irregular shape among the studied basins and is therefore considered less susceptible to flooding. Basin 17, with the maximum R_c value of 0.56, is relatively more circular in shape compared to Basin 17, which implies more flood susceptibility. In the flood susceptibility analysis based on the NMFI results, the distribution of circularity ratio values across the 24 basins is as follows: 9 basins the low susceptibility category (0.00–0.25), 6 basins the moderate susceptibility category (0.25–0.50), 5 basins the high susceptibility category (0.50–0.75), and 4 basins are classified as very high susceptibility (0.75–1.00; Figure 5).

3.2.6. Compactness coefficient (C_c)

This parameter is another morphometric index used to determine whether basins have a circular geometry. A C_c value approaching 1 indicates that the drainage basin has a more circular shape and a higher potential for flood generation, while values farther from 1 correspond to more elongated basins with lower flood potential. In this study, C_c values range from 1.34 to 3.28. Basin 17 has the lowest C_c value of 1.34, indicating the highest flood potential, whereas Basin 24, with the highest value of 3.28, shows the lowest flood potential. According to the NMFI method, the flood susceptibility classification of the basins is as follows: 2 basins are in the low susceptibility class (0.00–0.25), 5 basins in the moderate class (0.25–0.50), 5 basins in the high class (0.50–0.75), and 12 basins the very high susceptibility class (0.75–1.00; Figure 6).

3.3. Relief Parameters (B_h)

3.3.1. Basin relief

Basin relief is a morphometric parameter that represents the elevation difference between the maximum and minimum points within a drainage basin. This parameter helps to understand whether a basin has a rugged or relatively flat topography. Such topographic characteristics significantly influence fluvial erosion and transport processes, particularly in terms of water conveyance capacity, erosional dynamics, and flood potential (Strahler, 1964; El-Fakharany & Mansour, 2021). Basin 22, with a relief value of 1015 meters, represents a lower and less rugged topography compared to the other basins. In contrast, Basin 24, with a relief value of 2240 meters, exhibits a highly rugged and elevated topography, which corresponds to a higher potential for flooding. This substantial relief suggests that runoff will be much faster in Basin 24, as the significant elevation difference will cause water to move quickly. Based on the NMFI results, the flood susceptibility classifications for the 24 basins in terms of basin relief (B_h) are as follows: 4 basins low susceptibility category (0.00–0.25), 5 basins moderate susceptibility category (0.25–0.50), 11 basins high susceptibility category (0.50–0.75), 4 basins are classified as very high susceptibility (0.75–1.00; Figure 6).

3.3.2. Ruggedness number (R_n)

Ruggedness number quantifies the structural complexity and relief of a basin by combining slope and elevation range (Melton, 1957). In this study, R_n values range from 3.19 to 45.12, indicating significant variation in terrain characteristics. Basin 24, with the highest Rn (45.12), represents highly rugged and steep terrain, which enhances surface runoff, reduces infiltration, and increases the likelihood of flash floods (Rai et al., 2018; Sutradhar & Mondal, 2023). On the other hand, Basin, with the lowest Rn (1.7), reflects relatively smooth and low-relief topography where runoff is slower, but prolonged rainfall may still cause water accumulation and localized flooding. In this study, based on the NMFI results, the flood susceptibility classifications for the basins in terms of Ruggedness Number (R_n) are as follows: 17 basins the low susceptibility category (0.00–0.25), 5 basins the moderate susceptibility category (0.25–0.50), 1 basin is classified as high susceptibility (0.50–0.75), 1 basin is in the very high susceptibility category (0.75–1.00; Figure 6).

3.3.3. Hypsometric integral (H_i)

It provides insights into the stage of landscape evolution and can help in assessing the degree of erosion a region has undergone (Strahler, 1952). Basins 18 with higher H_i values (e.g., 0.61) are characterized by steep slopes and high relief, resulting in limited infiltration and rapid surface runoff, thereby increasing the likelihood of flash floods. Conversely, basins 6 with lower H_i values (e.g., 0.15) exhibit more subdued topography and greater potential for water storage, yet they may still be prone to pluvial flooding, especially in areas where natural drainage has been altered by urbanization or land use changes. Based on NMFI method, 6 basins the low (0.00–0.25), 5 basins moderate (0.50–0.75), 7 basins high (0.50–0.75), and 6 basins has the very high flood susceptibility classes (0.75–1.00; Figure 6).

3.3.4. Gradient ratio (R_g)

This parameter is an important factor showing the average gradient of the river basin and the flood potential of the basin (Sreedevi et al., 2005). The Gradient Ratio (R_g) values in the 24 drainage basins under examination range from 0.03 to 0.19. This indicates the basins that emerge from the Amanos Mountains have different slopes. The steep slopes of Basin 17, which has a maximum R_g value of 0.19, increase surface runoff and raise the risk of flooding. In contrast, Basin 22, which has the lowest gradient ratio, represents a gentler topography and corresponds to lower flood susceptibility. According to the NMFI method, the distribution of flood susceptibility is as follows: 3 basins the low (0.00–0.25), 13 into the moderate (0.25–0.50), 3 into the high (0.50–0.75), and 5 into the very high flood susceptibility category (0.75–1.00; Figure 6).

3.3.5. Times of concentration (T_c)

The time of concentration (T_c) is defined as the time taken for surface runoff water to travel from the most distant point of a basin to its outlet. In the study of 24 basins, T_c values range from 0.63 to 4.04 hours. Basin 17 has the shortest time of concentration, while Basin 22 has the longest. Basins with shorter T_c values allow water to accumulate rapidly within the basin, increasing flood potential, whereas basins with longer T_c values generally have a lower flood risk. The NMFI results for T_c are as follows: 1 basin is categorized as having low flood susceptibility (0.00–0.25), 3 basins are in the moderate flood susceptibility category (0.25–0.50), 5 basins are classified as high flood susceptibility (0.50–0.75), 15 basins are classified as very high flood susceptibility (0.75–1.00; Figure 6).

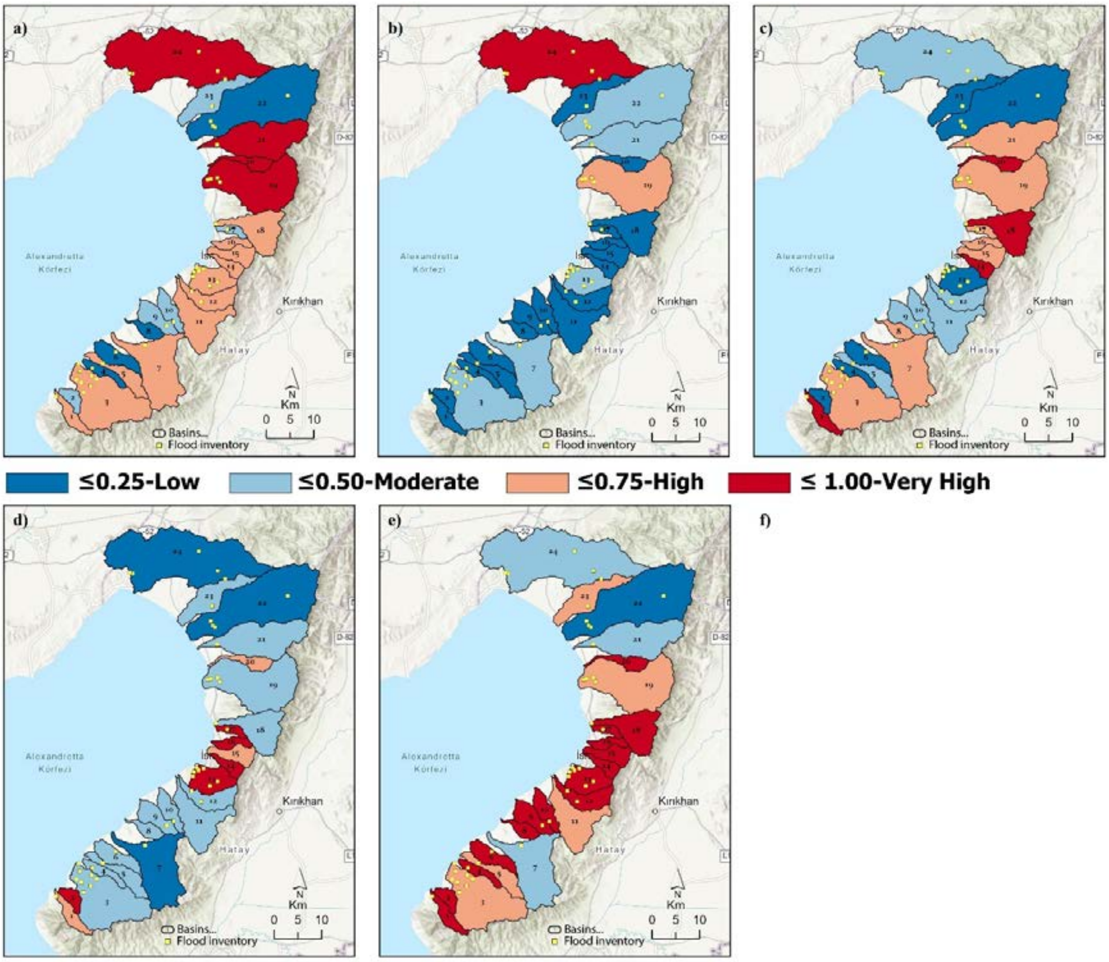

Figure 6: Normalised value distributions of the relief morphometric parameters a) B_h, b) R_n, c) H_i, d) Rg, and e) T_c evaluated for the flood-generating potential of the İskenderun Körfezi River basins.

3.4. Quantitative summary of morphometric indicators

Table 2 presents the descriptive statistical properties of 16 morphometric parameters derived from 24 drainage basins. Table 2 presents the descriptive statistical properties of 16 morphometric parameters derived from the analysis of 24 drainage basins. The mean values indicate that both the bifurcation ratio (R_b) and stream number (R_n) have the highest averages (0.8162), reflecting a strong influence of branching patterns within the drainage networks. On the other hand, the lowest mean values were observed for D_d and T_c (0.2075). These results generally indicate that the basins have relatively sparse drainage networks and rapid surface runoff responses. Similarly, the standard deviation and variance results provide important insights into the variability among the 24 river basins. Among these, L_o, F_s, and the form factor indices stand out, as they play a decisive role in final drainage conditions and reflect significant morphological characteristics related to basin geometry. In contrast, the R_b, R_n, and D_d indices exhibit low variance. Examination of the skewness values reveals negative skewness for Rb, Rn, Hi, and L_o, indicating that most values are concentrated toward the upper end of the scale, with a few lower outliers. In contrast, positive skewness in parameters such as D_d, F_s, R_e, and T_c implies that most basin values cluster toward the lower end, with a few higher values pulling the mean upward. Kurtosis analysis reveals pronounced peakedness for several parameters. Notably, R_b, R_n, and T_c exhibit high positive kurtosis (leptokurtic distribution), particularly Rb and R_n (kurtosis = 18.12), suggesting sharply peaked distributions with heavy tails. This indicates that extreme values are more frequent for these parameters. Other variables like L_o and R_c display slightly negative kurtosis, indicating flatter (platykurtic) distributions with lighter tails and more uniform spread.

Table 2: Descriptive summary of morphometric variables characterizing the study area.

	Mean	Std. Deviation	Variance	Skewness	Kurtosis
R_b	0.8162	0.185	0.034	-3.986	18.12
L_o	0.6125	0.321	0.103	-0.578	-1.001
T	0.2946	0.286	0.082	1.181	0.425
D_d	0.2075	0.239	0.057	1.933	4.332
F_s	0.3088	0.297	0.088	0.977	-0.201
R_e	0.3792	0.269	0.072	0.783	-0.042
R_f	0.4538	0.236	0.056	0.372	0.25
C_c	0.6542	0.264	0.07	-0.786	-0.013
R_c	0.4275	0.283	0.08	0.381	-0.757
B_h	0.5225	0.282	0.079	-0.175	-0.232
R_n	0.8162	0.185	0.034	-3.986	18.12
H_i	0.6125	0.321	0.103	-0.578	-1.001
R_g	0.2946	0.286	0.082	1.181	0.425
T_c	0.2075	0.239	0.057	1.933	4.332

3.5. Correlogram Analysis of Morphometric Parameters

The correlogram reveals statistically significant and strong linear relationships among several morphometric parameters (Figure 7). The correlation analysis of morphometric parameters shows important relationships between basin shape and drainage characteristics. A very strong positive correlation was found between stream frequency (T) and stream density (F_s) ($r = 0.97$), meaning that more streams per area are linked to a denser drainage system. Likewise, drainage density (D_d) and stream number (R_n) are also strongly correlated ($r = 0.94$), indicating that basins with more drainage channels tend to have higher density. The circularity ratio (R_c) and compactness coefficient (C_c) also show a very high correlation ($r = 0.94$), which suggests both describe similar aspects of basin shape. Total stream length (R_g) is highly related to stream number (R_n) (r = 0.86), showing the close link between stream quantity and overall drainage length. Several negative correlations were also observed. For example, the compactness coefficient (C_c) and drainage density (D_d) have a strong negative relationship (r = -0.89), suggesting that basins with dense drainage are usually less compact. The same applies to stream frequency (T) and time of concentration (T_c) (r = -0.83); basins with more frequent streams tend to have shorter response times. In addition, stream density (F_s) and compactness (C_c) are negatively correlated (r = -0.85), reinforcing this pattern. With regards to the main channel length (L_o), both stream frequency (F_s), drainage density (D_d) and its value show moderate to strong positive correlations. Accordingly, there is a significant correlation between the final drainage development and the shape of the basin. On the other hand, no correlation was found between R_e, F_s, and D_d, and these results indicate that elongated (elliptical) basins have a simpler and more organized drainage network and system. Using the correlogram, it is easier to understand the interdependency of morphometric parameters. While some values can be deemed supportive and developmental towards each, others exhibit opposing tendencies. These trends are vital to basin shape and hydrology correlation theory development. Furthermore, they can aid in watershed management as well as in flood risk analysis.

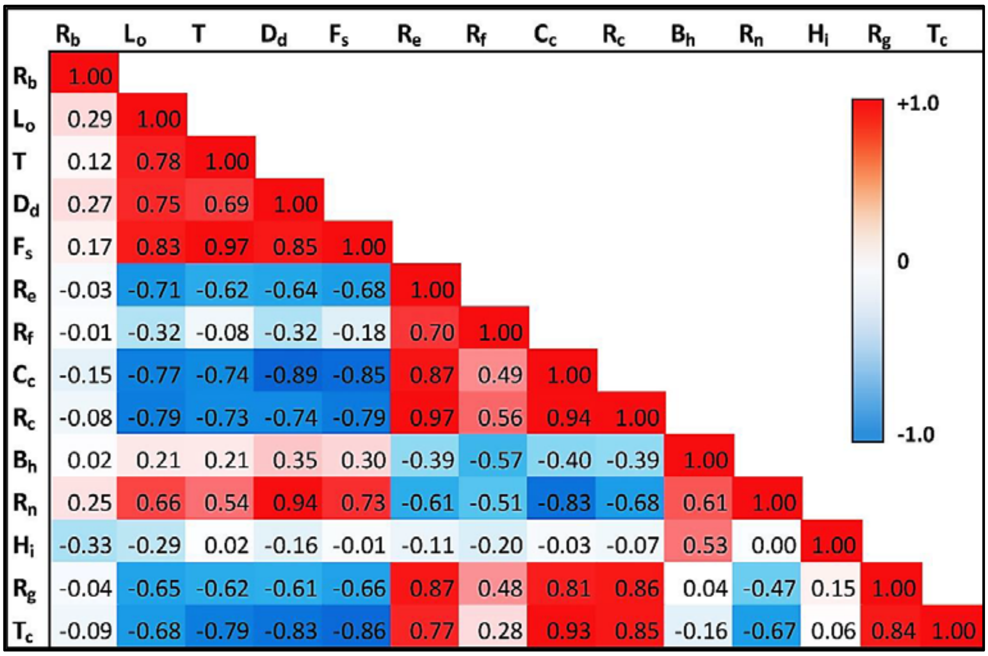

Figure 7: Morphometric parameters displayed as a correlogram, where positive relationships are highlighted in shades of red, and negative relationships appear in shades of blue.

3.6. Results

3.6.1. Multivariate Evaluation of Basin Morphometry: Results from NMFI and PCA Approaches

In this section, flood susceptibilities of 24 river basins were evaluated using two different multivariate methods NMFI and PCA.

3.6.1.1. Normalized Morphometric Flood Index (NMFI) Results

Employing the NMFI technique, the present flood susceptibility of 24 basins was evaluated with the aid of 14 different morphometric geomorphic indices considered as linear, areal and relief parameters. These parameters R_b, L_o, T refer to linear morphometry, D_d, F_s, R_e, R_f, C_c, R_c refer to areal morphometry and Bh, Rn, Hi, R_g, T_c pertains to relief morphometry. All parameters were normalized so their values would range from 0 to 1. Based on Ozdemir and Akbas (2023), these values were categorized into: Low (0.00–0.25), Moderate (0.25–0.50), High (0.50–0.75), and Very High (0.75–1.00) flood susceptibility level. This final NMFI value was derived by averaging the 14 parameters. This tells us that there is no absolute standard for judging the flood risk potential across basins and it is subjective. The outcome showed that 15 sub-basins were in the Moderate range of flood susceptibility while 9 sub-basins showed a higher level of flood susceptibility. In the moderate category, basins numbered 1, 4-12, 21-24 suggests a morphometric oriented level of low to moderate flood chance. On the other hand, basins 2, 3, and 13–19 were identified as having high susceptibility, reflecting more pronounced morphometric features conducive to rapid runoff, steeper gradients.

3.6.1.2. Principal Component Analysis (PCA) Results

Principal Component Analysis (PCA) was applied to minimize data dimensionality and to elucidate the major axes of variation among the morphometric indices. The analysis extracted four principal components with eigenvalues exceeding 1, as summarized in Table 3.

Table 3 presents the eigenvalue distribution for each extracted component. In accordance with the Kaiser criterion (eigenvalues>1), four components were retained for further interpretation. Component 1, accounting for 48.28% of the total variance (Eigenvalue = 8.29), exhibited strong positive loadings on variables such as C_c (0.98), R_c (0.95), T_c (0.91), and Rg (0.82). These associations emphasize the dominant influence of areal and relief morphometric parameters on basin response. Conversely, notable negative loadings on L_o (−0.85), T (−0.82), Dd (−0.89), F_s (−0.91), and R_n (−0.83) indicate an inverse relationship between drainage density, texture, and basin elongation with flood susceptibility.

Component 2, explaining 18.07% of the total variance (Eigenvalue=2.01), primarily reflects relief-related parameters such as B_h (−0.76) and H_i (−0.80). Component 3 (13.45% of variance; Eigenvalue = 1.27) and Component 4 (10.58% of variance; Eigenvalue = 1.09) represent secondary variation patterns with comparatively weaker or mixed parameter contributions, as detailed in Table 3.

Table 3: a) Total variance explained of the morphometric indices, b) Rotated component matrix.

Component	Initial Eigenvalues			Extraction Sums of Squared Loadings			Rotation Sums of Squared Loadings				Component			
a)	Total	% of Variance	Cumulative %	Total	% of Variance	Cumulative %	Total	% of Variance	Cumulative %	b)	1	2	3	4
1	8.29	59.21	59.21	8.29	59.213	59.213	6.759	48.28	48.28	R_l	-0.18	0.38	0.71	-0.24
2	2.01	14.34	73.55	2.007	14.336	73.55	2.53	18.071	66.35	L_o	-0.85	0.27	0.10	-0.03
3	1.27	9.06	82.61	1.269	9.061	82.611	1.884	13.454	79.804	T	-0.82	0.22	-0.09	0.43
4	1.09	7.78	90.39	1.089	7.775	90.386	1.481	10.582	90.386	D_d	-0.89	0.13	0.26	0.09
5	0.58	4.12	94.51							F_s	-0.91	0.17	0.03	0.36
6	0.42	3.03	97.54							R_e	0.89	0.21	0.24	0.25
7	0.14	1.03	98.56							R_f	0.51	0.59	-0.02	0.59
8	0.12	0.88	99.44							C_c	0.98	0.04	0.02	0.00
9	0.05	0.32	99.77							R_c	0.95	0.10	0.18	0.10
10	0.02	0.13	99.90							B_h	-0.41	-0.76	0.42	0.14
11	0.01	0.09	99.99							R_n	-0.83	-0.15	0.41	0.02
12	0.00	0.01	99.99							H_i	0.02	-0.80	-0.14	0.42
13	0.00	0.01	100.00							R_g	0.82	-0.17	0.43	0.29
14	0.00	0.00	100.00							T_c	0.91	-0.17	0.19	-0.10

3.6.2. Comparison of PCA and NMFI -Based Flood Susceptibility Classifications

The classification results derived from both the Principal Component Analysis (PCA) and the Normalized Morphometric Flood Index (NMFI) methods exhibit a high degree of similarity. According to the NMFI approach, 8 watersheds were classified as having high flood susceptibility, while 16 watersheds were categorized under moderate susceptibility. In the PCA-based classification, 6 watersheds were identified as highly susceptible, and 18 were deemed moderately susceptible (Figure 8). Notably, no watersheds were assigned to either low or very high susceptibility classes in either method. The overlapping results between the two methods indicate a strong agreement and reinforce the reliability of morphometric parameters in flood susceptibility assessment. Specifically, the following watersheds were consistently identified as highly susceptible in both methods: 3, 13, 14, 17 and 19. Additionally, the watersheds classified as having moderate susceptibility in both approaches include: 1, 4, 5, 6, 7, 8, 9, 10, 11, 12, 16, 20, 22, 23, and 24 (Figure 8). These correspondences confirm the stability and consistency of the susceptibility patterns derived from two independent analytical frameworks. Such agreement suggests that PCA, like NMFI, effectively captures the dominant geomorphometric characteristics governing flood dynamics across the study area.

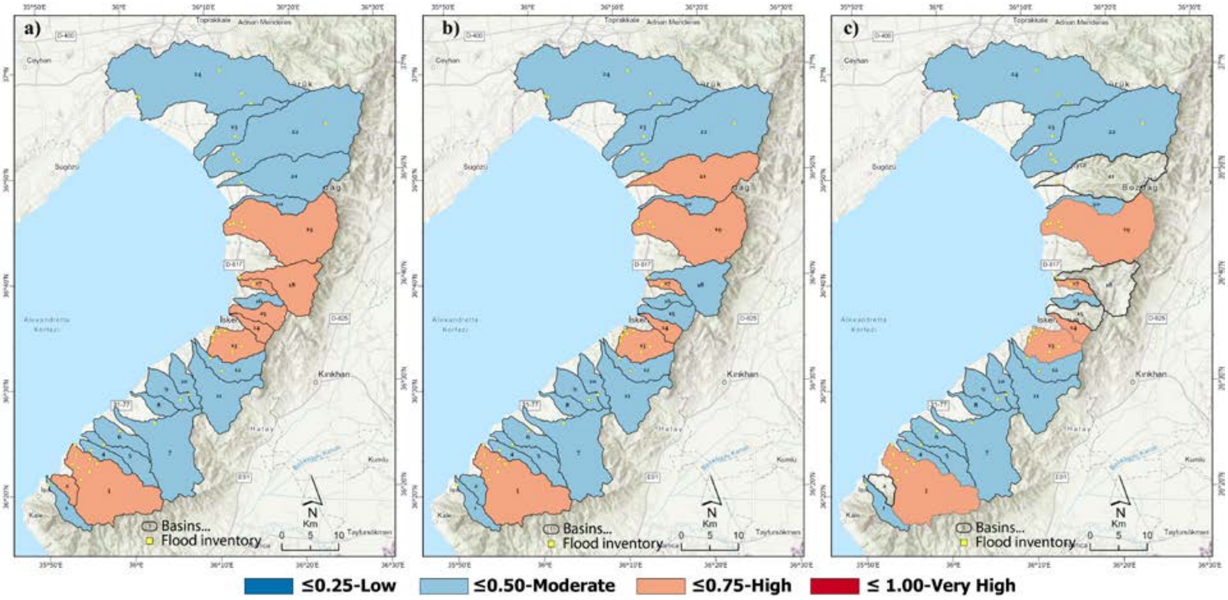

Figure 8: a) NMFI result, b) PCA result, and c) common basins.

3.6.3. Evaluation of the Results

Two flood susceptibility assessment methods (Normalized Morphometric Flood Index and Principal Component Analysis) were applied and evaluated using classification performance metrics, including true positive (TP), true negative (TN), false positive (FP), false negative (FN), recall (TPR), F1-score, specificity (TNR), accuracy, and Matthews Correlation Coefficient (MCC). The NMFI method identified 5 true positives and 1 true negative, but also produced a high number of false negatives (18), leading to a relatively low recall (0.217) and moderate F1-score (0.357). While NMFI achieved perfect specificity (1.0), its overall classification performance was weak, with an accuracy of only 0.25 and an MCC of 0.230, indicating a limited correlation between predictions and actual outcomes (Figure 9a-b). On the other hand, the PCA method achieved improved predictive results with 7 true positives and only 16 false negatives. PCA showed better recall (0.304), F1-score (0.466), and accuracy (0.333), along with similarly perfect specificity (1.0). Its MCC value (0.296) reflected a slightly stronger correlation than NMFI, suggesting more reliable prediction capabilities. In summary, while both methods exhibited high specificity, PCA outperformed NMFI in terms of overall classification metrics, demonstrating better balance and reliability in identifying flood-prone basins.

a)

	NFMI				PCA			
	TP	TN	FP	FN	TP	TN	FP	FN
N	5	1	0	18	7	1	0	16
P	1.0				1.0			
TPR (Recall/Sensivity)	0.217				0.304			
F1-Score(F)	0.357				0.466			
Specificity (TNR)	1.0				1.0			
Accuracy	0.250				0.333			
Matthews Corr. Coef (MCC)	0.230				0.296			

b)

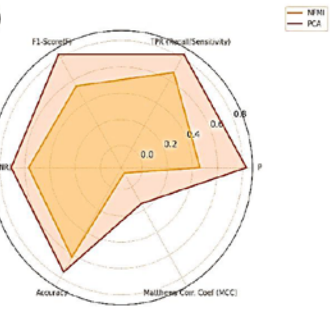

Figure 9: a) Classification metrics derived from confusion matrices for NMFI and PCA methods, and b) Radar chart illustrating comparative model performance across key metrics.

4. CONCLUSION

In this study, flood events that have occurred in 24 river basins flowing east to west and originating from the Amanos Mountains were analyzed based on basin-scale flood morphometry. The flood susceptibility classes were determined using two statistical methods: the Normalized Morphometric Flood Index (NMFI) and Principal Component Analysis (PCA). The results obtained from both methods were then validated using historical flood inventory data to test their accuracy. Flood susceptibility classifications, which were identified based on the physical characteristics of the basins, such as geometric form, drainage structure, and relief, were also empirically evaluated to assess their validity.

Unlike other methodologies, the NMFI approach is straightforward to use and interpret; however, it was not effective at successfully identifying basin regions that are highly susceptible to flooding. This is due to the fact that the NMFI approach only relies on normalized values and does not attempt to explore the relationships between geomorphometric indices. Perhaps these are the reasons for inadequate results. Another approach is identified as PCA. It gathers the most useful information as it removes some variables, thus ensuring more consistent, reliable, accurate results. As a result, the classification achieved through PCA proved more efficient in overcoming challenges to measure recall and precision, specificity, F1 score, and total accuracy. Although the outcomes demonstrate a significant improvement, the results suggest that the PCA-based approach offers a more reliable means of delineating flood-prone regions while minimizing misclassification errors. Both susceptibility models were validated against a flood inventory compiled from extensive field observations, providing an empirical basis for model comparison. The evaluation revealed that classifications produced using the PCA framework showed a markedly stronger correspondence with observed flood occurrences than those generated by the alternative model. Furthermore, flood-prone zones identified through the PCA method exhibited a clearer hierarchical structure consistent with documented field evidence.

Beyond its predictive accuracy, the application of PCA also elucidated the relative influence of key morphometric parameters, thus offering valuable insights into the underlying physical controls of flood susceptibility within the study area. Beyond its methodological contributions, the study underscores the importance of integrating morphometric analysis with environmental and anthropogenic data for more robust flood risk modeling. While topographic characteristics provide a valuable foundation, variables such as land use, vegetation cover, rainfall intensity, soil infiltration capacity, and hydraulic critically influence flood dynamics. The absence of these factors in purely morphometric models may limit the predictive scope in complex or rapidly urbanizing basins. From a practical standpoint, the study's outputs offer a spatially explicit, scientifically grounded decision-making tool for local planners and policymakers. Identifying the most flood-sensitive basins can guide the prioritization of structural and non-structural mitigation strategies, such as early warning systems, sustainable drainage planning, and zoning regulations. Furthermore, the use of open-source GIS tools and remotely sensed data enhances the replicability and scalability of the approach for other flood-prone regions.

In conclusion, this research demonstrates that the integration of PCA with morphometric analysis can significantly enhance the classification of flood-prone basins, offering both methodological innovation and applied value. Future studies should aim to build on this framework by incorporating dynamic environmental variables and conducting time-series analyses to capture seasonal and long-term trends in flood behavior. Additionally, in the process of implementing necessary mitigation measures, the rapid and effective application of hydraulic modeling in the field plays a critical role in enhancing the understanding of water flow directions during flood events. These models significantly contribute to interpreting current conditions more accurately, particularly when supported by high-resolution digital surface data derived from LiDAR and UAV (Unmanned Aerial Vehicle) technologies, which offer substantial advantages in terms of spatial detail and precision.

KAYNAKÇA

Alam, A., Ahmed, B., & Sammonds, P. (2021). Flash flood susceptibility assessment using the parameters of drainage basin morphometry in SE Bangladesh. Quaternary International,575–576:295–307. https://doi.org/10.1016/j.quaint.2020.04.047

Alifujiang, Y., Abuduwaili, J., Groll, M., Issanova, G., & Maihemuti, B. (2021). Changes in intra-annual runoff and its response to climate variability and anthropogenic activity in the Lake Issyk-Kul Basin, Kyrgyzstan. CATENA, 198:104974. https://doi.org/10.1016/j.catena.2020.104974

Arabameri, A., Tiefenbacher, J.P., Blaschke, T., Bradhan, B., & Bui, D.T. (2020). Morphometric analysis for soil erosion susceptibility mapping using novel GIS-based ensemble model. Remote Sensing, 12:874. https://doi.org/10.3390/rs12050874

Arnell, N.W., & Gosling, S.N. (2016). The impacts of climate change on river flood risk at the global scale. Climatic Change, 134:387–401. https://doi.org/10.1007/s10584-014-1084-5

Aydin, O., & Raja, N.B. (2020). Spatial-temporal analysis of precipitation characteristics in Artvin, Turkey. Theoretical and Applied Climatology, 142:729–741. https://doi.org/10.1007/s00704-020-03346-6

Balcı, E., Bilgen, G., & Aksoy, S.H. (2024). Flood risk awareness and transportation mode choice in communities with varying flooding frequencies: The cases of Bozkurt, Kastamonu, Turkey and Malanday, Marikina, Philippines. International Journal of Disaster Risk Reduction, 113:104819. https://doi.org/10.1016/j.ijdrr.2024.104819

Bashir, B., & Alsalman, A. (2024). Characteristics and comparative assessment of flash flood hazard evaluation techniques: Insights from Wadi Haily Basin, Eastern Red Sea Coast, Saudi Arabia. Water (Switzerland), 16. https://doi.org/10.3390/w16243634

Bhat, M.S., Alam, A., Ahmad, S., Shah, H.F., & Ahmad, B. (2019). Flood hazard assessment of upper Jhelum basin using morphometric parameters. Environmental Earth Sciences, 78:1–17. https://doi.org/10.1007/s12665-019-8046-1

Demirbilek, S., & Turoğlu, H. (2025). Arsuz Çayı Havzası'nın sel duyarlılık analizi. Doğu Coğrafya Dergisi, 30(53), 96-111. https://doi.org/10.17295/ataunidcd.1629115

Dickie, G. (2022). Floods, other water-related disasters could cost global economy $5.6 trillion by 2050 -report, Reuters

DSİ. (2012). Annual flood reports

El-Fakharany, M.A., & Mansour, N.M. (2021). Morphometric analysis and flash floods hazards assessment for Wadi Al Aawag drainage Basins, southwest Sinai, Egypt. Environmental Earth Sciences, 80:1–17. https://doi.org/10.1007/s12665-021-09457-1

Enea, A., Stoleriu, C. C., Iosub, M., & Niacsu, L. (2024). A GIS Automated Tool for Morphometric Flood Analysis Based on the Horton–Strahler River Classification System. Water, 16(4), 536. https://doi.org/10.3390/w16040536

Farhan, Y., Anbar, A., Al-Shaikh, N., & Mousa, R. (2017). Prioritization of semi-arid agricultural watershed using morphometric and principal component analysis, remote sensing, and GIS techniques, the Zerqa River Watershed, Northern Jordan. Agricultural Science, 08:113–148. https://doi.org/10.4236/as.2017.81009

Ghasemlounia, R., & Utlu, M. (2021). Flood prioritization of basins based on geomorphometric properties using principal component analysis, morphometric analysis and Redvan's priority methods: A case study of Harşit River basin. Journal of Hydrology, 603:127061. https://doi.org/10.1016/j.jhydrol.2021.127061

Gravelius, H. (1914). Grundrifi der gesamten Gewcisserkunde. Band I: Flufikunde (Compendium of Hydrology, Vol. I. Rivers, in German). Goschen, Berlin.

Gürer, İ., & Uçar, İ. (2009). Flood Disasters' Inventory in Turkey in 2009. Elev Int Symp Water Manag Hydraul Eng 371–380

Haltas, I., Yildirim, E., Oztas, F., & Demir, I. (2021). A comprehensive flood event specification and inventory: 1930–2020 Turkey case study. International Journal of Disaster Risk Reduction, 56:102086. https://doi.org/10.1016/j.ijdrr.2021.102086

Hirabayashi, Y., Kanae, S., Emori, S., Oki, T., & Kimoto, M. (2008). Global projections of changing risks of floods and droughts in a changing climate. Hydrological Sciences Journal, 53:754–772. https://doi.org/10.1623/hysj.53.4.754

Hirabayashi, Y., Mahendran, R., Koirala, S., Konoshima, L., Yamazaki, D., Watanabe, S., Kim, H., & Kanae, S. (2013). Global flood risk under climate change. Nature Climate Change, 3:816–821. https://doi.org/10.1038/nclimate1911

Horton, R.E. (1945). Erosional development of streams and their drainage basins: hydrophysical approach to quantitative morphology. Bulletin of the Geological Society of America 56, 2 75-3 70. Prog Phys Geogr Earth Environ 19:533–554. https://doi.org/10.1177/030913339501900406

Horton, R.E. (1932). Drainage-basin characteristics. Trans Am Geophys Union 13:350. https://doi.org/10.1029/TR013i001p00350

Kirpich, Z. P. (1940). Time of concentration of small agricultural watersheds. Journal of Civil Engineering, 10(6), 362.

Koç, G., Petrow, T., ve Thieken, A. H. (2020). Analysisof the most severe flood events in Turkey (1960-2014): Which triggering mechanisms andaggravating pathways can be identified? Water (Switzerland), 12(6), 1–32. https://doi.org/10.3390/W12061562

Kowalzig, J. (2008). Climate, Poverty, and Justice: What the Poznan UN climate conference needs to deliver for a fair and effective global deal. Oxfam Policy Pract Clim Chang Resil 4:117–148

Kumar Rai, P., Narayan Mishra, V., & Mohan, K. (2017). A study of morphometric evaluation of the Son basin, India using geospatial approach. Remote Sensing Applications: Society and Environment, 7:9–20. https://doi.org/10.1016/j.rsase.2017.05.001

Mayer, L. (1990) Introduction to Quantitative Geomorphology. Prentice Hall, Englewood Cliffs.

Melton, M. (1957). An analysis of the relation among elements of climate, surface properties and geomorphology. Office of Naval Research Technical Report No. 11, (11), 99. New York

Milly, P., Wetherald, R.T., Dunne, K.A., & Delworth, T. (2002). Increasing risk of great floods in a changing climate. Nature, 415:514–517. https://doi.org/10.1038/415514a

Mishra, A.K., & Rai, S.C. (2020). Geo-hydrological inferences through morphometric aspects of the Himalayan glacial-fed river: a case study of the Madhyamaheshwar River basin. Arabian Journal of Geosciences, 13:533. https://doi.org/10.1007/s12517-020-05571-9

Obeidat, M., Awawdeh, M., & Al-Hantouli, F. (2021). Morphometric analysis and prioritisation of watersheds for flood risk management in Wadi Easal Basin (WEB), Jordan, using geospatial technologies. Journal of Flood Risk Management, 14:1–19. https://doi.org/10.1111/jfr3.12711

OECD. (2016). Financial Management of Flood Risk, First Edit. OECD Publishing, Paris. https://doi.org/10.1787/9789264257689-en

Özay, B., & Orhan, O. (2023). Flood susceptibility mapping by best–worst and logistic regression methods in Mersin, Turkey. Environ Sci Pollut Res 30:45151–45170. https://doi.org/10.1007/s11356-023-25423-9

Özdemir, H., & Akbaş, A. (2023). Is there a consistency in basin morphometry and hydrodynamic modelling results in terms of the flood generation potential of basins? A case study from the Ulus River Basin (Türkiye). Journal of Hydrology, 625:129926. https://doi.org/10.1016/j.jhydrol.2023.129926

Pike, R. J., & Wilson, S. E. (1971). Elevation-relief ratio, hypsometric integral, and geomorphic area-altitude analysis. Bulletin of the Geological Society of America, 82(4), 1079–1084.

Rai, P.K., Chandel, R.S., Mishra, V.N., & Singh, P. (2018). Hydrological inferences through morphometric analysis of lower Kosi river basin of India for water resource management based on remote sensing data. Applied Water Science, 8:1–16. https://doi.org/10.1007/s13201-018-0660-7

Rai, P.K., Singh, P., Mishra, V.N., Singh, A., Sajan, B., & Shahi, A.P. (2020) Geospatial approach for quantitative drainage morphometric analysis of varuna river basin, India. Journal of Landscape Ecology, 12:1–25. https://doi.org/10.2478/jlecol-2019-0007

Rentschler, J., Salhab, M., & Jafino, B.A. (2022). Flood exposure and poverty in 188 countries. Nat Commun 13:1–11. https://doi.org/10.1038/s41467-022-30727-4

Schumm, S.A. (1956). Evolution of drainage systems and slopes in badlands at Perth Amboy, New Jersey. GSA Bull 67:597–646. https://doi.org/10.1130/0016-7606(1956)67[597:EODSAS]2.0.CO;2

Smith, K. G. (1950). Standards for grading texture of erosional topography. American Journal of Science, 248(9), 655–668. https://doi.org/10.2475/ajs.248.9.655

Sreedevi, P.D., Subrahmanyam, K., & Ahmed, S. (2005). The significance of morphometric analysis for obtaining groundwater potential zones in a structurally controlled terrain. Environmental Geology, 47:412–420. https://doi.org/10.1007/s00254-004-1166-1

Strahler, A.N. (1952). Hypsometric (area-altitude) analysis of erosional topography. Bulletin of the Geological Society of America, 63:1117–1142

Strahler, A. N. (1958). Dimensional analysis applied to fluvially eroded landforms. GSA Bulletin, 69(3), 279–300. https://doi.org/10.1130/0016-7606(1958)69[279:DAATFE]2.0.CO;2

Strahler, A.N. (1964). Quantitative geomorphology of drainage basins and channel networks. In: Chow, V., Ed., Handbook of Applied Hydrology, McGraw Hill, New York, 439-476.

Sutradhar, S., & Mondal, P. (2023). Prioritization of watersheds based on morphometric assessment in relation to flood management: A case study of Ajay river basin, Eastern India. Watershed Ecology and the Environment, 5:1–11. https://doi.org/10.1016/j.wsee.2022.11.011

Taşoğlu, E., Öztürk, M. Z. & Yazıcı, Ö. (2024). High Resolution Köppen-Geiger Climate Zones of Türkiye. International Journal of Climatology, 44(14), 5248-5265.

Tayanç, M., İm, U., Doğruel, M., & Karaca, M. (2009). Climate change in Turkey for the last half century. Climatic Change, 94:483–502. https://doi.org/10.1007/s10584-008-9511-0

Telore, N. V. (2020). Quantitative Morphometric Analysis of the Yerla River Basin, Deccan Trap Region, India. Içinde: Sahdev S, Singh RB, Manish K (ed) In Geoecology of Landscape Dynamic, First. Singapore, ss 115–132

Trenberth, K.E. (2011). Changes in precipitation with climate change. Climate Research, 47:123–138. https://doi.org/10.3354/cr00953

Tukura, N.G., Akalu, M.M., Hussein, M., & Befekadu, A. (2021). Morphometric analysis and sub-watershed prioritization of Welmal watershed, Ganale-Dawa River Basin, Ethiopia: implications for sediment erosion. Journal of Sedimentary Environments, 6:121–130. https://doi.org/10.1007/s43217-020-00039-y

Utlu, M., Şimşek, M., & Öztürk, M. Z. (2020). 1D Taşkin Modellemeleri Açisindan Topo Dem ve Alos Dsm Verilerinin Karşilaştirilmasi: Alara Çayi Örneği. Ege Coğrafya Dergisi, 29(2), 161-177. https://dergipark.org.tr/tr/pub/ecd/issue/58525/775152

Utlu, M., & Ghasemlounia, R. (2021). Flood Prioritization Watersheds of the Aras River, Based on Geomorphometric Properties: Case Study Iğdır Province. Jeomorfolojik Araştırmalar Dergisi (6), 21-40. https://doi.org/10.46453/jader.781152

Utlu, M. (2023). Frekans Oranı ve Shannon Entropisi Yöntemi Kullanarak Ezine Çayı Havzası Taşkın Duyarlılık Analizi (Kastamonu-Bozkurt). Jeomorfolojik Araştırmalar Dergisi (11), 160-178. https://doi.org/10.46453/jader.1358845

Youssef, A.M., Pradhan, B., & Hassan, A.M. (2011). Flash flood risk estimation along the St. Katherine road, southern Sinai, Egypt using GIS based morphometry and satellite imagery. Environmental Earth Science, 62:611–623. https://doi.org/10.1007/s12665-010-0551-1

Yüksek, Ö., Kankal, M., & Üçüncü, O. (2013). Assessment of big floods in the Eastern Black Sea Basin of Turkey. Environmental Monitoring and Assessment, 185:797–814. https://doi.org/10.1007/s10661-012-2592-2

Url-1 https://worldcover2021.esa.int/viewer

Url-2 https://www.iha.com.tr/haber-hatayda-sel-felaketi-426874

Url-3 https://www.aa.com.tr/tr/turkiye/cokek-yaylasinda-sel-heyelana-neden-oldu-5-olu/231351